

Solution Structures of Human Parathyroid Hormone Fragments hPTH(1–34) and hPTH(1–39) and Bovine Parathyroid Hormone Fragment bPTH(1–37)

Ute Charlotte Marx,^{*,†,1} Knut Adermann,[†] Peter Bayer,[‡] Wolf-Georg Forssmann,[†] and Paul Rösch^{*}

^{*}Lehrstuhl für Biopolymere, Universität Bayreuth, D-95440 Bayreuth, Germany; [†]Niedersächsisches Institut für Peptid-Forschung (IPF), Feodor-Lynen-Straße 31, D-30625 Hannover, Germany; and [‡]Max-Planck-Gruppe für Enzymologie der Proteinfaltung, Weinbergweg 22, D-01620 Halle/Saale, Germany

Received October 26, 1999

Parathyroid hormone (PTH) is involved in regulation of the calcium level in blood and has an influence on bone metabolism, thus playing a role in osteoporosis therapy. In this study, the structures of the human PTH fragments (1–34) and (1–39) as well as bovine PTH(1–37) in aqueous buffer solution under near physiological conditions were determined using two-dimensional nuclear magnetic resonance spectroscopy. The overall structure of the first 34 amino acids of these three peptides is virtually identical, exhibiting a short NH₂-terminal and a longer COOH-terminal helix as well as a defined loop region from His14 to Ser17, stabilized by hydrophobic interactions. bPTH(1–37), which has a higher biological activity, shows a better-defined NH₂-terminal part. In contrast to NH₂-terminal truncations, which cause destabilization of helical structure, neither COOH-terminal truncation nor elongation significantly influences the secondary structure. Furthermore, we investigated the structure of hPTH(1–34) in 20% trifluoroethanol solution. In addition to its helix-stabilizing effect, tri-

fluorethanol causes the loss of tertiary hydrophobic interactions. © 2000 Academic Press

Key Words: human parathyroid hormone; bovine parathyroid hormone; NMR; peptide structure.

This work was supported by grants from the Fonds der Chemischen Industrie (FCI) (to P.R.) and from Deutsche Forschungsgemeinschaft (DFG, BA-1624/3-1) (to P.B.).

Abbreviations used: bPTH, bovine parathyroid hormone; Clean-TOCSY, TOCSY with suppression of NOESY-type cross peaks; dgsa, distance geometry simulated annealing; COSY, correlated spectroscopy; DQF-COSY, double quantum filtered COSY; DG, distance geometry; DSS, 2,2-dimethyl-silapentane-5-sulfonic acid; DSSP, definition of secondary structure of proteins; HBTU, 2-(1H-benzotriazol-1-yl)-1,1,3,3-tetramethyluronium tetrafluoroborate; hPTH, human parathyroid hormone; MD, molecular dynamics; NOE, nuclear Overhauser effect, also used for NOESY cross peak; NOESY, NOE spectroscopy; ppm, parts per million; PTH, parathyroid hormone; rmsd, root-mean-square deviation; TFE, 2,2,2-trifluoroethanol; TOCSY, total correlation spectroscopy.

¹ To whom correspondence should be addressed at Lehrstuhl für Struktur und Chemie der Biopolymere, Universität Bayreuth, D-95440 Bayreuth, Germany. Fax: ++49 921 553544. E-mail: ute.marx@uni-bayreuth.de.

It is generally accepted that the NH₂-terminal 34 amino acids of the 84-amino-acid parathyroid hormone (hPTH) are sufficient for the known endocrine biological activities of this peptide hormone. The naturally occurring hPTH(1–37) fragment as well as hPTH(1–34) maintain normocalcemia in blood via adenylate cyclase activation (1). The involvement of the phosphatidylinositol hydrolysis signaling pathway is also postulated for this function (2). His14 to Phe34 is suggested to be the receptor binding region (3, 4), whereas the very NH₂-terminal part of the peptide is required for stimulation of the cAMP-dependent signal transduction pathway (2, 5). Furthermore, NH₂-terminal PTH fragments have an influence on cell proliferation in skeletal tissues (6) and on bone metabolism, thus playing an important role in osteoporosis therapy (7, 8). hPTH(1–34) is an intensely studied hPTH fragment as it contains these functional regions, and most NMR studies focused on this fragment (9–14). According to these studies, hPTH(1–34) shows a short NH₂-terminal helix and a longer COOH-terminal helix. No evidence for tertiary interactions was found in trifluoroethanol-containing solvent (10–13). The study by Barden and Kemp (9) on hPTH(1–34) in the absence of trifluoroethanol (TFE) contrasts partly the structure of naturally occurring hPTH(1–37) determined in aqueous buffer solution under near physiological conditions (15). In particular, the helix lengths and several long range interactions differ. The long range interactions between Leu15 and Trp23 (15) are confirmed by Pellegrini *et al.* (14) but their structure calculations,



however, did not result in a defined loop region from His14 to Ser17.

In this study, we investigate the structure of hPTH(1–34) in TFE-free aqueous buffer solution as well as in the presence of 20% TFE to study the influence of TFE on the secondary and tertiary structure of hPTH(1–34). As NH₂-terminal truncations of hPTH(1–37) led to a significant loss of secondary structure in the NH₂-terminal part of the peptide (16) it is of interest to investigate the influence of COOH-terminal truncation and elongation on secondary structure. Therefore, we determined the structure of hPTH(1–39) under near physiological conditions for comparison with that of hPTH(1–37) (15) and hPTH(1–34). Since the first 39 amino acids are highly conserved in parathyroid hormones from different organisms, the hPTH(1–39) fragment was selected for this study. Furthermore, we present the first structure of bovine PTH (bPTH), which is a favored model for the study of biological activity and receptor binding ability of PTH (6, 17–21). bPTH(1–34) has a 2.4-fold higher adenylate cyclase activation potency compared to hPTH(1–34), whereas the receptor binding affinity is equivalent (22). The structure of bPTH(1–37), which has three amino acid exchanges at position 1, 7, and 16 compared to hPTH(1–37), was determined under the same aqueous buffer conditions as that one of hPTH(1–37) (15).

MATERIALS AND METHODS

Peptide synthesis. Peptides were synthesized using standard Fmoc chemistry with HBTU activation as reported earlier (15, 16). All peptides were purified by reversed-phase HPLC. Peptide identity and purity was checked by HPLC, electrospray mass spectrometry, and amino acid analysis.

CD spectroscopy. CD spectra were recorded at 20.1°C in 0.5 mm cells from 250 to 190 nm at 20 nm/min on a Jasco J 600A CD spectropolarimeter. Peptide concentrations ranged from 77.3 to 93.1 μM in 10 mM phosphate buffer, pH 6.2 with 50 mM sodium chloride in 200 ml volume. Additionally, hPTH(1–34) was dissolved in 10 mM phosphate buffer, pH 6.2, with 20% TFE. The reference sample contained buffer without peptide. Four scans were accumulated from samples and reference, respectively.

NMR spectroscopy. NMR spectra were recorded on a Bruker AMX600 spectrometer at 25.0°C. The measurements of hPTH(1–34), hPTH(1–39), and bPTH(1–37) in aqueous buffer solution were carried out in 50 mM phosphate buffer, with 270 mM sodium chloride. Peptide concentrations were: 4.0 mM, pH 6.0 for hPTH(1–34), 2.2 mM, pH 5.8 for hPTH(1–39) and 1.7 mM, pH 6.1 for bPTH(1–37) in H₂O/D₂O (9:1, v/v, 500 ml). Additionally, hPTH(1–34) was dissolved in H₂O/TFE-d₂ (4:1, v/v, 500 ml), 50 mM phosphate buffer (pH 6.0 before addition of TFE) with a final peptide concentration of 2.4 mM. The H₂O resonance was presaturated by continuous coherent irradiation at the H₂O resonance frequency prior to the reading pulse. The spectra were recorded with a spectral width of 7042.3 Hz in both dimensions and 4 K × 0.5 K data points in the time domain. Quadrature detection was used in both dimensions with the time proportional phase incrementation technique in ω₁. Spectra were multiplexed with a squared sinebell function phase shifted by π/4, π/3 or π/2 for the NOESY (mixing time 200 ms), the Clean-TOCSY (mixing time 80 ms) and the DQF-COSY spectra, respectively, prior to Fourier transformation. Application of zero filling resulted in 4 K ×

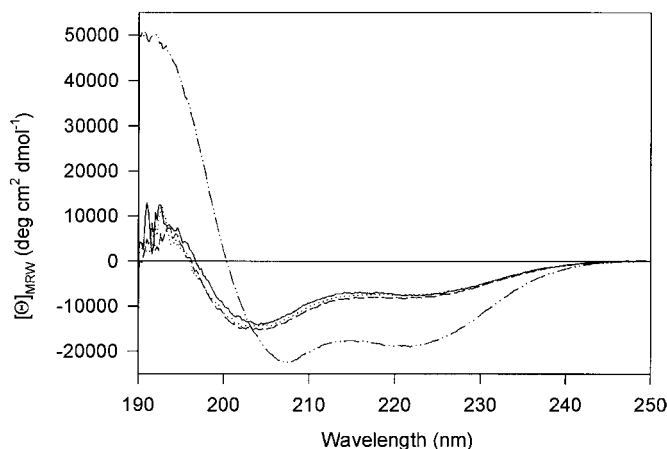


FIG. 1. Far UV CD spectra of hPTH(1–34) (—), hPTH(1–39) (---), bPTH(1–37) (···) in aqueous buffer solution, respectively, and hPTH(1–34) in 20% TFE solution (- · · -).

1 K data points in the frequency domain. Sixth order baseline and phase correction were used. Data were evaluated on X-window workstations with the NDee program package (Software Symbiose, Bayreuth).

Restrained molecular dynamics calculations. Distance geometry (DG) and molecular dynamics (MD) calculations were performed with the X-PLOR 3.1 program package (23) on a HP735 computer. The number of nontrivial interresidual NOESY cross peaks used for structure calculation was 206 for hPTH(1–34), 188 for hPTH(1–39) and 200 for bPTH(1–37) under aqueous conditions. In TFE-containing solution, 219 interresidual NOEs for hPTH(1–34) were assigned (Table I). These cross peaks were divided into three groups according to their relative intensities: strong, 0.2 to 0.3 nm, medium, 0.2 to 0.4 nm, and weak, 0.2 to 0.5 nm. 0.05 nm was added to the upper distance limit for distances involving unresolved methyl or methylene proton resonances. The structure calculations followed standard procedures employing a hybrid DG-restrained MD approach with simulated annealing refinement and subsequent energy minimization [protocol dgsa (23)]. For the refinement, the dielectric constant ϵ was set to 4. Structure parameters were extracted from the standard parallhdg.pro and topallhdg.pro files (24). For each fragment, 30 structures were calculated. 10 structures for every fragment were selected on the criteria of smallest number of NOE violations more than 0.05 nm and lowest overall energy.

Structure analysis. The final structures were analyzed with respect to stable idealized elements of regular secondary structure using the DSSP (definition of secondary structure of proteins) program package (25). To elucidate the stability of the structures we calculated the local root-mean-square deviation (rmsd) with a five amino acid window (26). For visualization of structure data SYBYL 6.0 (TRIPOS Association) and Raster3D (27) were used.

The ensembles of 10 structures of each fragment have been deposited in the Brookhaven Protein Data Bank, accession numbers: fragments under aqueous near physiological experimental conditions, hPTH(1–34), 1ZWA; hPTH(1–39), 1BWV; hPTH(1–37), 1HPH; bPTH(1–37), 1ZWC; and hPTH(1–34) in 20% TFE solution, 1HPY.

RESULTS AND DISCUSSION

The overall shapes of the circular dichroism (CD) spectra indicate the presence of both α -helical and random coil structural elements (28, 29) for all PTH fragments (Fig. 1). The evaluation of the spectra of

hPTH(1–34), hPTH(1–39), and bPTH(1–37) in aqueous buffer solution using standard methods (28, 30) yields estimated helix contents of about 27% each. This corresponds to 9 to 11 residues per peptide in a helical conformation on time average. For hPTH(1–34) in 20% TFE solution 56% α -helix were estimated, corresponding to 19 residues in helical conformation on time average.

Using homonuclear two-dimensional ^1H NMR spectroscopy the sequence specific resonance assignment could be performed with standard techniques (31) for all fragments, except for the spin systems of Ala1 and Glu19 of bPTH(1–37). For a first estimation of the localization of regions with defined secondary structure, the C_α -proton chemical shifts were analyzed according to the chemical shift index strategy by Wishart *et al.* (32, 33), allowing a qualitative comparison of the helix content of the different peptides. From this procedure two helical regions were suggested for hPTH(1–34) and hPTH(1–39) in aqueous buffer solution: from Glu4 to at least His9, with an upfield shift of the C_α -proton resonances up to His14, and from Ser17 to at least Gln29 (Figs. 2a and 2b). The COOH-terminal helix is more stable than the NH_2 -terminal one, indicated by a more pronounced upfield shift of the C_α -proton resonances. No other elements of regular secondary structure could be estimated by this method. The C_α -proton chemical shifts from Ser1 to His32 (except Leu28, 0.03 ppm difference) of hPTH(1–34) are identical within 0.02 ppm, which is in the margin of experimental error, with those of hPTH(1–37) under the same experimental conditions (15). The C_α -proton chemical shifts of hPTH(1–39) are identical within 0.02 ppm with the C_α -proton chemical shifts of hPTH(1–37) from Ser1 to Val31. The additional upfield shift for His32 and Phe34 to Ala36 is insufficient to indicate an elongation of the COOH-terminal helix. Thus, the backbone conformations of these three human peptides are expected to be virtually identical under aqueous solution conditions.

The addition of 20% TFE to hPTH(1–34) instead of buffer and salt solution results also in the estimation of two helical regions (Fig. 2d): the NH_2 -terminal helix is lengthened from Glu4 to His14, confirming the helix propensity as deduced from the upfield shifts of the C_α -proton resonances observed in TFE-free solution (Fig. 2a). The location and length of the COOH-terminal helix is the same as under aqueous conditions, but the stability of both helices is increased. The C_α -proton chemical shifts of both termini and the region around Leu15 were not affected on addition of TFE, indicating that TFE only stabilizes α -helical structure in regions of potential helix propensity.

The C_α -proton chemical shifts of bPTH(1–37) in aqueous solution also suggest the existence of two helical regions, from Glu4 to His14 and from Ser17 to at least Gln29 (Fig. 2c). Compared to hPTH(1–37), the

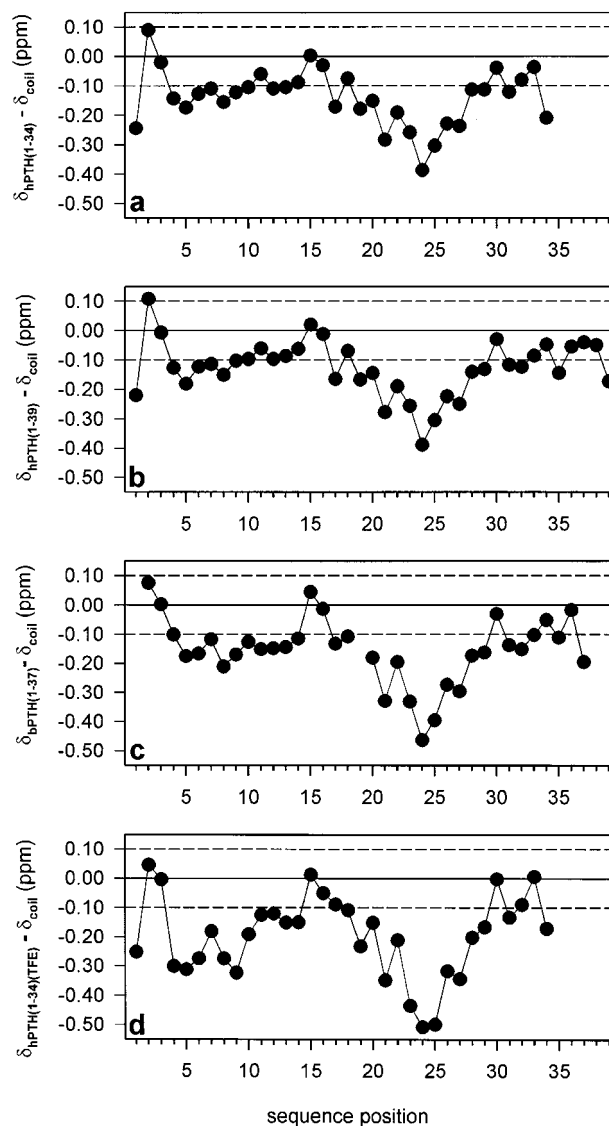


FIG. 2. Difference values of the observed C_α -proton chemical shifts relative to the “random coil” values according to Wishart *et al.* (33). The threshold of ± 0.1 ppm is indicated by dashed lines. (a) hPTH(1–34), (b) hPTH(1–39), (c) bPTH(1–37) in aqueous buffer solution (d) hPTH(1–34) in 20% TFE solution; for Gly12 the average value of both C_α -proton resonances is used.

C_α -proton resonances from Gln6 to His14 and from Met18 to Gln29 of bPTH(1–37) are shifted upfield, indicating increased helix stability for these regions of the bovine peptide.

Helix typical medium range $d_{\alpha\text{N}}(i, i + 3)$ and $d_{\alpha\beta}(i, i + 3)$ NOESY cross peaks corroborate the existence of two helical regions for hPTH(1–34), hPTH(1–39), and bPTH(1–37) in aqueous buffer solution (Figs. 3a–3c). In particular, $(i, i + 3)$ NOEs are clustered from Ile5 to Gly12 and Ser17 to Val31 for hPTH(1–34), from Ile5 to Leu11 and Ser17 to Phe34 for hPTH(1–39), and from Ser3 to Leu11 and from Ser17 to Phe34 for bPTH(1–37). Possible $(i, i + 3)$ NOEs for amino acids beyond

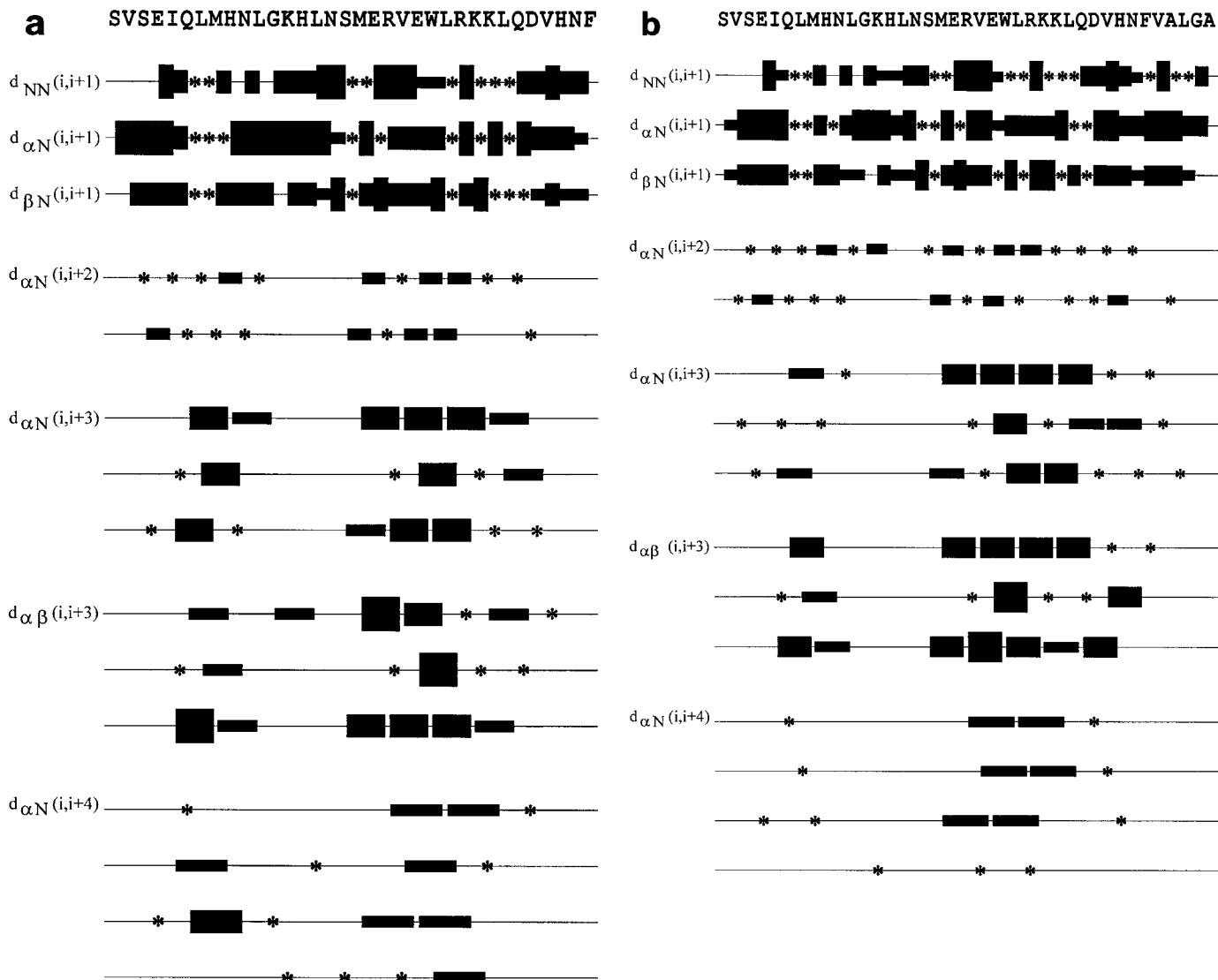


FIG. 3. Patterns of sequential and medium range NOE cross peaks versus peptide sequences. The height of the bars corresponds to the relative strength of the NOESY cross peaks. An asterisk indicates that the NOE could not be unambiguously assigned because of frequency degenerations. (a) hPTH(1-34), (b) hPTH(1-39), (c) bPTH(1-37) in aqueous buffer solution (d) hPTH(1-34) in 20% TFE solution.

Phe34 were lacking or could not be observed due to frequency degeneration (Figs. 3b and 3c). From the chemical shift indexes, a stable helical structure is not expected for amino acids downstream Gln29 for hPTH(1-34), and downstream His32 for hPTH(1-39) and bPTH(1-37) (Figs. 2a-2c). The relative intensities of the sequential and medium range NOEs of the three PTH-fragments investigated in TFE-free solution (Figs. 3a-3c) indicate that the helices are not ideal but are in an equilibrium with a more extended conformation, possibly a 3_{10} -helix. The NH_2 -terminal helices seem to have a higher tendency to a more extended conformation. This phenomenon is also reflected by values of the upfield shift of the C_α -proton resonances (Figs. 2a-2c). The NOESY spectrum of hPTH(1-34) in 20% TFE shows helix typical $(i, i + 3)$ NOEs over the

whole stretch of the peptide from Val2 to Asp30, albeit only weak ones around Leu15. Medium and strong helix typical NOEs are clustered from Val2 to His14 and from Ser17 to Asp30 (Fig. 3d). In this regions the relative intensities of the medium range $d_{\alpha\beta}(i, i + 3)$ NOEs are increased on addition of TFE whereas the intensities of the sequential $d_{\alpha\text{N}}(i, i + 1)$ NOEs are decreased, indicating an increased stability of both helices (Figs. 3a and 3d).

TFE not only influences the secondary, but also the tertiary structure of hPTH(1-34). All three PTH fragments in TFE-free solution show several long range NOEs between Leu15 and Trp23. This spatial proximity is most probably caused by hydrophobic interaction between these two residues. The $\text{C}\delta$ -proton resonances of Leu15 are shifted upfield in comparison to the anal-

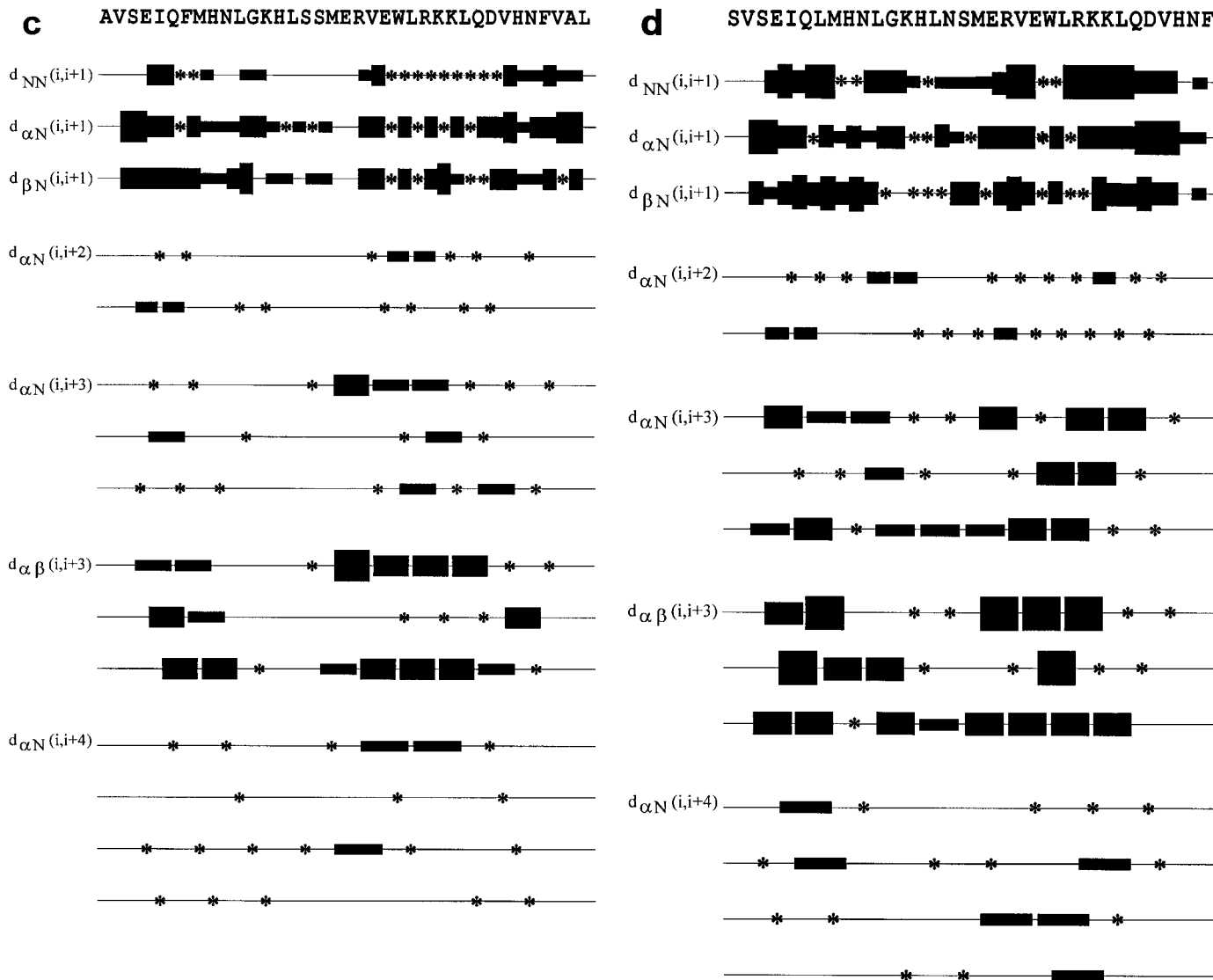


FIG. 3—Continued

ogous resonances of other leucines for all three fragments, possibly due to the ring current field of the spatially neighboring aromatic ring system of Trp23. In TFE-containing solution, no upfield shift is found for the $C\delta$ -proton resonance of Leu15. It appears that the spatial proximity to the aromatic system of Trp23 is lost.

For structure calculations, 188 to 219 interresidual NOEs per fragment were collected from 200-ms NOESY spectra at 298 K (Table I) and used in restrained MD calculations with a combined distance geometry/simulated annealing protocol (23). The structures of hPTH(1–34), hPTH(1–39), and bPTH(1–37) in near physiological aqueous buffer solution are very similar to that of hPTH(1–37) under identical conditions (15), showing a short NH_2 -terminal helix around Gln6 to His9, a longer COOH-terminal helix, Met18 to

at least Gln29, connected by a flexible hinge around Gly12, and a defined loop region from His14 to Ser17. The observed long range NOEs between Leu15 and Trp23 are responsible for a restriction of the conformational space of the calculated structures of all three fragments in the absence of TFE. These structural features of the hPTH peptides in TFE-free solution are also reflected by the local rmsd using a five amino acid window (26), as the regions with defined structure show substantially reduced local rmsd values compared to the flexible regions at the termini and around Leu11/Gly12 (Figs. 4a and 4b). Under identical near physiological conditions, the structures of hPTH(1–34) and hPTH(1–39) are virtually identical to the structure of hPTH(1–37) (15). Neither COOH-terminal truncation [hPTH(1–34)] nor elongation [hPTH(1–39)] have a drastic effect on the stability of the secondary structure

TABLE I

Energy Contributions to the Structures and Deviations from Standard Geometry, NOE, and X-PLOR Statistics

Number of NOEs	hPTH(1-34)	hPTH(1-39)	bPTH(1-37)	hPTH(1-34) (20% TFE)
Total	206	188	200	219
$ i - j = 1$	111	115	117	125
$ i - j = 2$	16	12	13	19
$ i - j = 3$	56	45	43	62
$ i - j = 4$	17	12	13	13
$ i - j = 5$	3	1	6	0
$ i - j > 5$	3	3	8	0
Average energies (kJ/mol)				
E_{total}	-1365.69	-2764.39	-976.88	-1642.91
E_{bonds}	314.87	260.23	320.45	254.99
E_{angles}	573.51	386.86	659.96	567.88
E_{impr}	126.07	62.06	137.98	87.16
E_{VDW}	-2267.72	-2927.14	-2114.64	-2347.32
E_{NOE}	535.30	165.60	549.92	519.388
Deviations from standard geometry				
Bonds (nm)	0.0011	0.0010	0.0011	0.0010
Angles (deg)	0.9194	0.7175	0.9522	0.8968
impr (deg)	0.7984	0.5358	0.8051	0.6668
NOEs (nm)	0.0111	0.0064	0.0114	0.0106
NOE violations > 0.05 nm				
	≤4	≤1	≤4	≤4
rmsd among backbone structures (nm)				
Whole peptide	0.469	0.442	0.463	0.366
Met18-Leu28	0.062	0.051	0.072	0.035
His14-Leu28	0.092	0.088	0.109	0.131

Note. Number and type of the unambiguously assigned interresidual NOEs used for structure calculations. E_{total} , total energy; E_{VDW} , van der Waals energy; E_{NOE} , effective NOE energy term resulting from a square-well potential function. All calculations were carried out using the standard X-PLOR force field and energy terms. The values are mean values over 10 refined structures for each peptide.

of the peptides, in contrast to our findings for NH_2 -terminal truncated forms of hPTH(1-37), hPTH(3-37) and hPTH(4-37), for which the NH_2 -terminal helix is lost in parallel with the biological activity (16). The structural identical hPTH fragments hPTH(1-34) and hPTH(1-37), which show both helices and the loop region, have the same *in vivo* biological activity using Parsons' chicken assay (16, 34).

For the 10 final structures of hPTH(1-34) in 20% TFE two helical regions were identified by DSSP analysis (25): from Glu4 to Lys13/His14 and from Met18 to Gln29. For the residues between the helices turn or bend structure was assigned, and one structure shows a continuous helix from Ile5 to Gln29. Not only the length of the NH_2 -terminal helix, but also the stability of both helices is increased. Comparing the local rmsd values over a five amino acid window of hPTH(1-34) under the different solution conditions (Figs. 4a and 4d), the flexible hinge around Gly12 in the absence of TFE is shifted to Leu15/Asn16 on addition of TFE. The

flexibility around Gly12 is lost as this residue is part of the extended NH_2 -terminal helix. The restriction of the structure around Leu15, defined by Leu15/Trp23 NOEs under physiological conditions is lost because of the loss of the hydrophobic interactions between these residues on addition of TFE, indicated by the absence of an upfield shift of the $\text{C}\delta$ -proton resonances of Leu15. Possible long range NOEs between Leu15 and Trp23 in TFE-containing solution would be ambiguous because of frequency degeneration of the $\text{C}\delta$ -protons of Leu15 with those of other leucines. Structure calculations, however, show that the unambiguous additional (i, i + 3) NOEs in the midregion of the peptide in TFE-containing solution and hypothetical long range NOEs between Leu15 and Trp23 could not be fulfilled at the same time without an increase of the overall energy. Thus, this long range interaction is highly unlikely to exist in the presence of TFE. Comparison of the structures of hPTH(1-34) with and without addition of TFE shows that TFE exclusively stabilizes

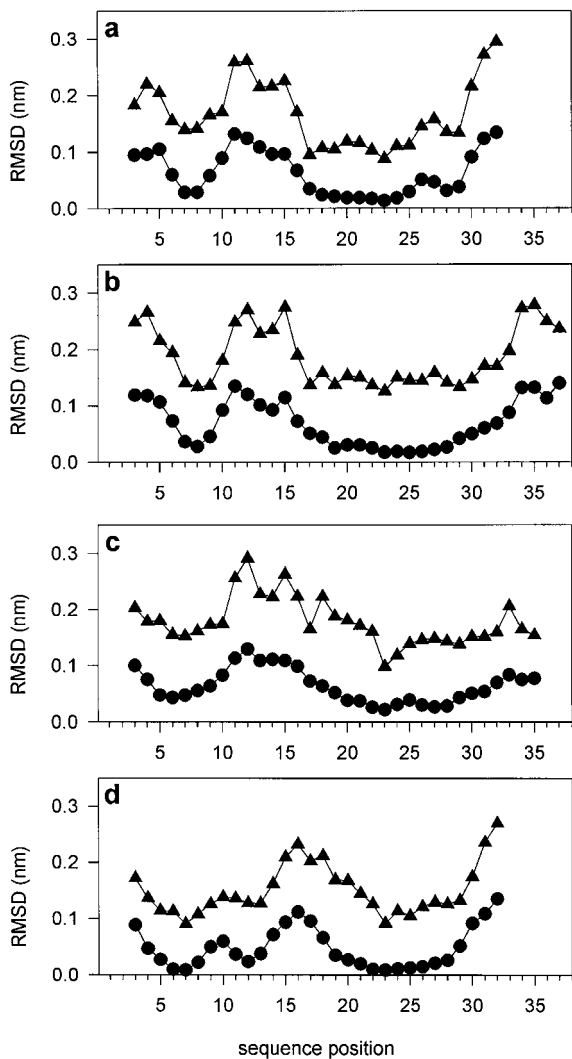


FIG. 4. Local rmsd values calculated with a five amino acid window (26). The plot was calculated on the basis of the 10 final structures of each PTH fragment. The upper trace describes the rmsd values for all heavy atoms, the lower trace describes the values for the peptide backbone. (a) hPTH(1–34), (b) hPTH(1–39), (c) bPTH(1–37) in aqueous buffer solution (d) hPTH(1–34) in 20% TFE-solution.

α -helical structure in regions which have an initial propensity of helix formation. In TFE-containing solution, however, the tertiary hydrophobic interactions between Leu15 and Trp23 are lost, so that it can be concluded that TFE destroys hydrophobic interactions within the peptide and, therefore, its native structure.

So far, most structure investigations of PTH fragments using NMR spectroscopy were carried out on hPTH(1–34) in TFE-containing solution (10–13). The most striking differences of these structures to the structure of hPTH(1–34) in TFE-free solution, that is a longer and more stable NH_2 -terminal helix and the missing of long range interactions, could be confirmed in the present work. hPTH(1–34) in aqueous solution

at pH 4.1 (9) and pH 4.3 (14) also exhibits NOEs between Leu15 and Trp23. Additional long range NOEs in the COOH-terminal part of the peptide and a longer and more stable NH_2 -terminal α -helix, as proposed by Barden and Kemp (9), could not be confirmed in our present and earlier work (15, 16) in near physiological aqueous buffer solution.

All investigated fragments under aqueous buffer conditions show the loop region and the COOH-terminal helix, which comprise the major part of the receptor binding region (3, 4), as well as the NH_2 -terminal helix. The *in vivo* biological activity of hPTH seems to be connected with the existence of the NH_2 -terminal helix (16). For the *in vitro* ability to stimulate adenylate cyclase the first amino acid seems to play a crucial role as hPTH(2–37) is nearly inactive in the adenylate cyclase assay (16). As bPTH(1–37) has a substitution of alanine for serine at position 1 and phenylalanine for leucine at position 7 in the NH_2 -terminal part, as well as serine for asparagine at position 16 compared to hPTH, a closer examination of the bPTH(1–37) structure (Fig. 4c, Fig. 5) may provide an explanation for its higher adenylate cyclase potency (22).

For bPTH(1–37) under near physiological conditions, an additional long range NOE was found between Val2 and Asn10, and (i, i + 5)-NOEs were found between Val2 and Phe7 (Fig. 5), indicating a more structured NH_2 -terminus for bPTH than for hPTH. This is reflected by a lower local rmsd value for the amino acids Val2 to Ile5 (Fig. 4c). The local rmsd value for the region from His14 to Leu28 of bPTH(1–37) is increased compared to the hPTH fragments under the same conditions (Table I, Fig. 4c), as these latter are better defined by NOEs. For all hPTH fragments, NOEs observed between side chain protons of Asn16 and Glu19

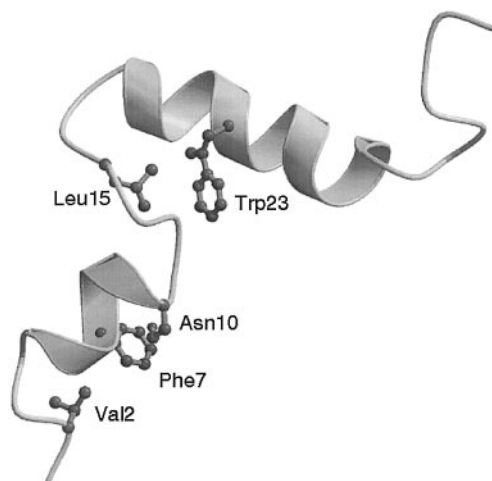


FIG. 5. Representative structure of bPTH(1–37). The helices are indicated as ribbons and the side chains of key residues are labeled. The figure was prepared with Raster3D (27).

may define a hydrogen bond between these side chains. For bPTH(1–37) Ser16 may also function as a hydrogen bond donor, but possible NOEs between Ser16 and Glu19 could not be observed, as the spin system of Glu19 of bPTH(1–37) could not be assigned. Thus, the conformational space in this region is not as good restricted as for the human PTH fragments (Table I). Irregularities in the loop region and the beginning of the COOH-terminal helix (Table I, Fig. 4c), which are part of the receptor binding region, can rather be ascribed to missing NOEs for the unassigned spin system of Glu19 of bPTH(1–37) than to inherent flexibility. The structure of bPTH(1–37) seems to be similar to that of hPTH(1–37) (15), with a more stable NH₂-terminal region (Fig. 5). The higher stability of the NH₂-terminal part of bPTH together with the amino acid exchange at position 1 may provide an explanation for the higher adenylate cyclase activity compared to hPTH, whereas the receptor binding affinity is equivalent (22).

REFERENCES

- Potts, J. T., Jr., Kronenberg, H. M., and Rosenblatt, M. (1982) *Adv. Protein Chem.* **35**, 323–396.
- Coleman, D. T., Fitzpatrick, A., and Bilezikian, J. P. (1994) *in The Parathyroids* (Bilezikian, J. P., Levine, M. A., and Marcus, R., Eds.), pp. 239–258, Raven Press, New York.
- Caulfield, M. P., McKee, R. L., Goldmann, M. E., Duong, L. T., Fisher, J. E., Gay, C. T., DeHaven, P. A., Levy, J. J., Roubini, E., Nutt, R. F., Chorev, M., and Rosenblatt, M. (1990) *Endocrinology* **127**, 83–87.
- Lopez-Hilker, S., Martin, K. J., Sugimoto, T., and Slatopolsky, E. (1992) *J. Lab. Clin. Med.* **119**, 738–743.
- Luck, M. D., Carter, P. H., and Gardella, T. J. (1999) *Mol. Endocrinol.* **13**, 670–680.
- Sömjen, D., Schlüter, K.-D., Wingender, E., Mayer, H., and Kaye, A. M. (1991) *Biochem. J.* **277**, 863–868.
- Turner R. T., Evans G. L., Cavolina J. M., Halloran B., and Morey-Holton E. (1998) *Endocrinology* **139**, 4086–4091.
- Lane, N. E., Sanchez, S., Modin, G. W., Genant, H. K., Pierini E., and Arnaud, C. D. J. (1998) *Clin. Invest.* **102**, 1627–1633.
- Barden, J. A., and Kemp, B. E. (1993) *Biochemistry* **32**, 7126–7132.
- Klaus, W., Dieckmann, T., Wray, V., Schomburg, D., Wingender, E., and Mayer, H. (1991) *Biochemistry* **30**, 6936–6942.
- Barden, J. A., and Cuthbertson, R. M. (1993) *Eur. J. Biochem.* **215**, 315–321.
- Strickland, L. A., Bozzato, R. P., and Kronis, K. A. (1993) *Biochemistry* **32**, 6050–6057.
- Wray, V., Federau, T., Gronwald, W., Mayer, H., Schomburg, D., Tegge, W., and Wingender, E. (1994) *Biochemistry* **33**, 1684–1693.
- Pellegrini, M., Royo, M., Rosenblatt, M., Chorev, M., and Mierke, D. F. (1998) *J. Biol. Chem.* **273**, 10420–10427.
- Marx, U. C., Austermann, S., Bayer, P., Adermann, K., Ejchart, A., Sticht, H., Walter, S., Schmid, F.-X., Jaenicke, R., Forssmann, W.-G., and Rösch, P. (1995) *J. Biol. Chem.* **270**, 15194–15202.
- Marx, U. C., Adermann, K., Bayer, P., Meyer, M., Forssmann, W.-G., and Rösch, P. (1998) *J. Biol. Chem.* **273**, 4308–4316.
- Cohen, F. E., Strewler, G. J., Bradley, M. S., Carlquist, M., Nilsson, M., Ericsson, M., Ciardelli, T. L., and Nissenson, R. A. (1991) *J. Biol. Chem.* **266**, 1997–2004.
- Fujimori, A., Cheng, S. L., Avioli, L. V., and Civitelli, R. (1992) *Endocrinology* **130**, 29–36.
- Blind, E., Bambino, T., and Nissenson, R. A. (1995) *Endocrinology* **136**, 4271–4277.
- Ishikawa, Y., Wu, L. N., Genge, B. R., Mwale, F., and Wuthier, R. E. (1997) *Bone Miner. Res.* **12**, 356–366.
- Schwartz, Z., Semba, S., Graves, D., Dean, D. D., Sylvia, V. L., and Boyan, B. D. (1997) *Bone* **21**, 249–259.
- Keutmann, H. T., Griscom, A. W., Nussbaum, S. R., Reiner, B. F., Goud, A. N., Potts, J. T., Jr., and Rosenblatt, M. (1985) *Endocrinology* **117**, 1230–1234.
- Brünger, A. T. (1993) X-PLOR Version 3.1., Howard Hughes Medical Institute and Yale University, New Haven, CT.
- Brooks, B. R., Bruccoleri, R. E., Olafson, B. D., States, D. J., Swaminathan, S., and Karplus, M. (1983) *J. Comput. Chem.* **4**, 187–217.
- Kabsch, W., and Sander, C. (1983) *Biopolymers* **22**, 2577–2637.
- Wagner, G., Braun, W., Havel, T. F., Schaumann, T., Go, N., and Wüthrich, K. (1987) *J. Mol. Biol.* **196**, 611–639.
- Merritt and Murphy (1994) *Acta Cryst.* **D50**, 869–873.
- Greenfield, N., and Fasman, G. (1969) *Biochemistry* **8**, 4108–4116.
- Schmid, F.-X. (1997) *in Protein Structure: A Practical Approach* (Creighton, T. E., Ed.), pp. 261–297, IRL Press, Oxford.
- Morrisett, J. D., David, J. S. K., Pownall, H. J., and Gotto, A. M. (1973) *Biochemistry* **12**, 1290–1299.
- Wüthrich, K. (1986) *NMR of Proteins and Nucleic Acids*, Wiley, New York.
- Wishart, D. S., Sykes, B. D., and Richards, F. M. (1992) *Biochemistry* **31**, 1647–1651.
- Wishart, D. S., Bigam, C. G., Holm, A., Hodges, R. S., and Sykes, B. D. (1995) *J. Biomol. NMR* **5**, 67–81.
- Parsons, J. A., Reit, B., and Robinson, C. J. (1973) *Endocrinology* **92**, 454–462.